This is an Accepted Manuscript of an article published by Taylor & Francis in Composite Interfaces in 2015, available online: http://dx.doi.org/10.1080/09276440.2015.1053753

A COMPARATIVE EVALUATION BETWEEN FLAT AND TRADITIONAL ENERGY DIRECTORS FOR ULTRASONIC WELDING OF CF/PPS THERMOPLASTIC COMPOSITES

I. Fernandez Villegas[a*], B. Valle Grande[a], H. E.N. Bersee[a], R. Benedictus[a]

[a]*Structural Integrity and Composites Group, Faculty of Aerospace Engineering, Delft University of Technology, Kluyverweg 1, 2629 HS Delft, The Netherlands*

**e-mail address of the corresponding author: I.FernandezVillegas@tudelft.nl*

Keywords: thermoplastic composites, plastic ultrasonic welding, energy directors

Abstract

Energy directors, responsible for local heat generation in ultrasonic welding, are neat resin protrusions traditionally moulded on the surfaces to be welded. This paper evaluates an alternative energy directing solution for ultrasonic welding of thermoplastic composites based on the usage of a loose flat layer of neat resin at the welding interface, referred to as 'flat energy director'. Analysis of dissipated power, displacement of the sonotrode, welding energy and time as well as weld strength compared to more traditional energy directing solutions showed that flat energy directors, which significantly simplify ultrasonic welding of thermoplastic composites, do not have any substantial negative impact in the welding process or the quality of the welded joints.

1. Introduction

Ultrasonic welding is a joining process very well suited for spot welding of thermoplastic composite structures. Among its main advantages are very high processing rates (welding times of several seconds) and straightforward process monitoring, as indicated in [1, 2]. In fact, modern ultrasonic welders provide power and displacement data that can be directly related to the physical phenomena occurring at the joining interface during the welding process [2]. Process monitoring can be used either for quality assessment or as a powerful tool for the definition of optimum processing conditions [3]. In order to concentrate heat generation at the welding interface, energy directors are required in ultrasonic welding. Traditionally, energy directors are matrix resin protrusions on the surfaces to be welded which are subjected to high cyclic strains during the welding process and hence heat up faster than the adherends. Energy directors are traditionally moulded on the surfaces of the composite adherends. This process usually adds an extra step to the manufacturing of the composite parts to be welded. Moreover, the shape, size and number of energy directors need to be optimized in order to achieve high-quality welds [4]. As already shown in recent work by I.F. Villegas [2,3], there is a much more simple solution for ultrasonic welding of thermoplastic composites based on the usage of flat energy directors. A flat energy director is a loose layer of neat resin placed at the welding interface prior to the welding process. Preferential heating of the flat energy director results from the lower compressive stiffness of the neat resin relative to the compressive stiffness of the composite adherends. Flat energy directors have been found to provide high and consistent weld quality in ultrasonic welding of carbon-fibre reinforced polyetherimide (CF/PEI) composites [3].

The main goal of the research in this paper was to assess whether the simplicity in manufacturing offered by the flat energy directors has any counteracting effect in the welding process. With this purpose, welding with flat energy directors was evaluated relative to the more traditional solutions depicted in Fig. 1. These were triangular ridges moulded on the surface of the bottom adherend (denoted by 4TM energy director hereafter), as proposed by other authors, and triangular ridges moulded on one loose stripe of neat resin (denoted by 4T hereafter). Although all these types of energy directors were used in previous work [2-5], a direct comparison such as the one presented in this paper had not been made available so far.. Individual carbon-fibre reinforced polyphenilene sulfide (CF/PPS) composite samples were ultrasonically welded in a lap shear configuration using these three different types of energy directors. Relationships between the feedback of the ultrasonic welder, namely power and displacement data, and the transformations occurring at the interface were analysed for the three cases and used to define optimum welding parameters. Weld strength, failure modes, welding time and energy were compared and discussed.

2. Experimental

The material used for this research was carbon-fibre reinforced polyphenylene sulfide (CF/PPS) thermoplastic composite with a five harness satin fabric reinforcement, provided by Ten Cate Advanced Composites in The Netherlands. Six-layer laminates with a $[(0/90)_3]_s$ stacking sequence and 1.92 mm nominal thickness were manufactured in a hot platen press at 320°C and 10 bar for 15 min. 101.6 mm-long and 25.4 mm-wide adherends were water-jet cut out of these laminates with their longer side parallel to the main apparent orientation of the fibres.

The energy directors were manufactured in a hot platen press with the processing parameters displayed in Table 1. Note that a temperature below the melting temperature of PPS was used in all cases in order to prevent excessive resin flow and void formation. An aluminium mould with four triangular ridges (90° at the apex of the triangles, 0.7 mm triangle height, 3.25 mm spacing between consecutive apexes) was used for the manufacturing of the 4T energy directors (four triangular ridges moulded on a loose resin stripe) and 4TM energy directors (four triangular ridges moulded on the bottom substrate). The size, shape and number of triangular ridges were decided upon based on previous optimization studies. PPS film was used for the manufacturing of the flat and 4T energy directors, whereas PPS powder was used for the manufacturing of the 4TM energy directors following previous work [6]. The final measured dimensions of the energy directors are also displayed in Table 1. During the moulding of the 4TM energy directors, excess resin powder was laid on the mould to ensure a proper connection between the triangular ridges and the substrates. As a result, a resin layer remained between the triangular ridges and the composite, as shown in Fig. 2. It must be noted that the resin in the 4TM energy directors showed a certain degree of oxidation given away by its somewhat brown colour. Likewise, the energy directors featured some porosity caused by insufficient compaction of the PPS powder, as seen in Fig. 2.

Individual samples were welded in a single-lap configuration with a 12.7 mm-long overlap using a 20 kHz Rinco Dynamic 3000 ultrasonic welder. This is a microprocessor-controlled welder that automatically adjusts the electrical power input in order to ensure constant amplitude throughout the welding process. A 40 mm-diameter cylindrical titanium sonotrode was used in this study. A custom-made clamping tool that prevents the samples from shifting and allows for vertical movement of the upper substrate during the squeezing of the energy director out of the welding interface [2,3] was used (Fig. 3). Both the flat and the 4T energy

directors were cut to the final dimensions, placed between the adherends prior to the welding process and attached to the bottom adherend with adhesive tape In the case of the 4T energy directors, the flat side of the energy director was placed on top of the bottom adherend with the triangular ridges facing up, as shown in Fig. 1. A custom-designed aligning tool was used to ensure that the triangular ridges were parallel to the shortest side of the adherend and always placed in the same location (which coincided with the location of the triangular ridges in the 4TM energy director). The 4TM energy director was already moulded to the bottom substrates and thus needed no further fixation. Based on previous work on ultrasonic welding of thermoplastic composites with flat energy directors [2], 500 N welding force and 86.2 µm peak-to-peak vibration amplitude were chosen as the baseline input parameters for the welding process (medium force, high amplitude) which led to intermediate welding times and intermediate dissipated power levels [2]. Also based on previous work, the solidification force and solidification time were chosen to be 1000 N and 4 s, respectively, in all the samples welded in this research. The welding process was displacement controlled, meaning that the duration of the ultrasonic vibration was indirectly controlled through the displacement of the sonotrode [2,3]. The word “travel” is used in this work to denote the target displacement in each welding process.

The welded samples were mechanically tested under static load according to ASTM D 1002 in a Zwick 250 kN universal testing machine and standard environmental conditions. The apparent lap shear strength of the samples was calculated by dividing the maximum load by the overlap area (i.e. 25.4 mm x 12.7 mm). Five samples were tested per set of welding conditions and average lap shear strength and standard deviation values were calculated. Optical microscopy was used to analyse cross sections of the welded samples. Naked eye was used for the observation of the fracture surfaces.

3. Results and discussion

3.1. Power and displacement curves

Figure 4 shows representative power and displacement curves during the vibration stage of the welding process for the flat energy director case. It must be noted that the power represented in that Figure, shown as a percentage of the total available power (3000 W), is the electrical power consumed by the piezoelectric converter to achieve constant-amplitude welding. As explained in [7], it is believed that only a relatively little fraction of this total power is effectively used for the welding process. However the different events identified in the power curve can be linked to physical changes occurring in the welding stack, as shown in [2], since all of the other elements affected by the vibration during the welding process (booster, sonotrode, welding jig and anvil) can be considered “inert” to the vibration relative to the welding stack. The displacement represented in Figure 4 is the downward displacement of the sonotrode relative to its position at the onset of the vibration. These power and displacement curves show the same features as the ones presented in [2] for ultrasonic welding of CF/PEI composites with flat energy directors, despite the intrinsic differences between PEI, amorphous thermoplastic resin, and PPS, semi-crystalline thermoplastic resin. Even though, welding of semi-crystalline thermoplastics can be expected to require higher energy than welding of amorphous thermoplastics in the same conditions [4], the physical phenomena taking place during the welding process and hence the features in the power and displacement curves can be expected to be similar. As discussed in detail in [2], the power and displacement curves divide the vibration phase of the welding process in five distinct stages in which different physical phenomena are observed at the welding interface. In stage

1_F, characterized by a continuous increase of the power without significant changes in the displacement, heating of the energy director occurs without any observable physical transformations at the welding interface. In stage 2_F, characterized by a decrease of the power without significant changes in the displacement, the energy director starts to locally melt as a hot-spot nucleation and growth process. In stage 3_F, characterized by a simultaneous increase of the power and the displacement, the whole energy director is molten and starts to flow. In stage 4_F, which features a power plateau and increasing displacement, first melting and flow in the composite adherends occurs in parallel with squeeze flow of the energy director. Finally, in stage 5_F, characterized by a power drop and still increasing displacement, melting and flow of the matrix in the bulk of the composite adherends occurs.

When more traditional, triangular energy directors are used, heating and melting of the energy director first occurs close to the tip of triangles as stated by Benatar and Gutowski in [1], owing to a higher cyclic strain that results from the decreased cross-sectional area, and progresses towards the base of the triangles. Fig. 5 shows how this melting behaviour can be observed in the power and displacement curves for a welding process with 4T energy director (i.e. a resin stripe with four triangular ridges moulded on one side). As indicated in Fig. 5, the vibration phase of the welding process can be now divided into 7 stages. Stage A_{4T}, characterised by no displacement of the sonotrode and power increase, corresponds to the heating of the triangular ridges, which, as mentioned already, is concentrated near their tips. Due to the high cyclic strains the triangular ridges undergo during the welding process as well as the high contact pressure and hence surface friction between the ridges and the adherend, this heating phase is considerably shorter than heating of the flat energy directors (approximately 50 ms versus approximately 250 ms). In stage B_{4T} the triangular ridges gradually melt and flow from their tip to their base. Consequently, the displacement of the

sonotrode increases in this stage from 0 to 0.4 mm, which is close to the original height of the triangles in the energy director. Since the volume of resin that needs to be heated up to its melting temperature increases as the melting process progresses from the tip to the bottom of the triangles, a gradual increase in the power is also observed in stage B_{4T}. In stages 1_{4T} and 2_{4T}, the displacement of the sonotrode drastically slows down. These are the stages where the flat part of the energy director progressively heats up and melts and, hence, they are comparable to stages 1_F and 2_F in the flat energy director process, although with a considerably shorter duration. This is believed to result from a certain pre-heating of the flat part of the energy director during stages A_{4T} and B_{4T} caused, on one of its sides, by heating and melting of the triangular ridges and, on the opposite side, by surface friction against the adherend. As well as in stage 2_F, power drops in stage 2_{4T} as a result of a gradual decrease of the area of the flat part of the energy director yet to be heated and melted. Stages 3_{4T}, 4_{4T} and 5_{4T} are comparable to stages 3_F, 4_F and 5_F, respectively. They are therefore characterized by flow of the energy director as a whole and melting of the resin in the uppermost and, later on, in deeper layers of the adherends.

Figs. 6 to 8 show cross-section micrographs of welds with their vibration phase interrupted at different stages in the process to illustrate the evolution of the welding interface in the case of the 4T energy director. In all cases a solidification phase at 1000 N for 4 s is applied after the vibration phase is finished. Fig. 6 corresponds to a weld interrupted within the first half of stage B_{4T}. Three main observations can be drawn from this Figure. Firstly, melting and flow occurs at the tips of the triangles, which consequently show a rounded shape. Secondly, some of the resin layers that compose the energy director tend to separate. This is caused by the fact that, as explained in Section 2, the 4T energy directors are manufactured from different layers of resin film at a temperature just below the melting temperature of PPS and thus the different

resin layers are not fully molten together. Thirdly, friction between the flat part of the energy director and the bottom adherend has not generated, at that moment in the process, any melting at that interface and hence the energy director only bonds to the top adherend. Towards the end of stage B_{4T} (Fig. 7) the energy director is almost fully re-compacted and the space between the adherends almost covered with resin (some minor gaps still remain). Likewise, the bottom adherend is bonded to the energy director indicating the occurrence of heat generation between the bottom adherend and the flat bottom of the energy director. Later on, late in stage 3_{4T} (Fig. 8), the thickness of the weldline has considerably diminished, indicating squeeze flow of the energy director. No gaps or voids can be observed anymore.

Attempting to define stages in the vibration phase of 4TM energy director welding based on events in the power and displacement curves proved to be challenging due to the lack of reproducibility of the power curves, as shown in Fig. 9. This is believed to result from the poor quality of the energy directors. However, the shape of the displacement curves was consistent and similar to those obtained in the case of 4T energy directors. One of the most remarkable parallelisms between the 4TM and the 4T displacement data is a temporary but significant decrease in the displacement rate in the neighbourhood of 0.4 mm displacement. In the 4TM case, this is attributed to the presence of a relatively thick layer of resin between the base of the triangular ridges and the surface of the bottom adherend due to manufacturing constraints (see Fig. 2). This resin layer is believed to heat up and progressively melt in a similar fashion as the resin stripe in the 4T energy director. However, the fact that this layer of resin is moulded onto the bottom adherend hinders any relative movement and hence the possibility of heat generation through surface friction at the interface between the resin layer and the bottom adherend. As a result, the time until significant flow occurs again is

substantially longer in the case of the 4TM energy directors (around 200 ms, see Fig. 9) than in the case of 4T energy directors (below 100 ms, see Fig. 5).

3.2. Welding output

According to our results presented in [3] for ultrasonic welding of CF/PEI composites with flat energy directors, optimum single lap shear strength (LSS) values (i.e. maximum average and minimum standard deviation) are obtained when travel is such that the vibration phase of the welding process stops towards the end of stage 4_F, as defined in Fig. 4. The applicability of this procedure to ultrasonic welding of CF/PPS composites with flat and 4T energy directors was demonstrated in the present work by welding and testing CF/PPS samples within stages 3_F, 4_F and 5_F (Fig. 4) and 3_{4T}, 4_{4T} and 5_{4T} (Fig. 5), respectively. Fig. 10 plots lap shear strength versus travel for the flat and 4T energy director cases. Figs. 11 and 12 show representative power and displacement curves for all the travel values considered in Fig. 10. In the case of flat energy directors an optimum LSS of 37.1±1.3 MPa was obtained for 0.30 mm travel (see Fig. 10), which falls within stage 4F (see Fig. 11). Similarly, in the case of 4T energy director and optimum LSS of 35.8±1.5 MPa was obtained for 0.73 mm travel (see Fig. 10), which falls within stage 4_{TA} (see Fig. 12).

Owing to the difficulties in defining stages in the power curves of 4TM energy directors , the optimum travel was selected based on the analysis of the cross-section micrographs of samples welded at different travel values. A travel of 0.75 mm, which resulted in a welding interface free of the original porosity of the energy director and thickness visually similar to that of the resin-rich areas in the composite adherends was selected. Samples with 4TM energy directors welded using 0.75 mm travel yielded a LSS that amounted to 17.7±4.6 MPa.

The fracture surfaces of these samples revealed mostly interfacial failure on the bottom adherend (see Fig. 13), indicating little to no melting on that surface. Conversely, extensive melting of the matrix with significant deformation of the fibre bundles can be observed in the mating surface fracture. This indicates that the heat generated in the triangular ridges is easily transferred to the adherend they are in direct contact with. On the contrary, the existence of a layer of resin between the ridges and the bottom adherend serves as an insulator that hinders heat transfer in that direction. Moreover, the lack of surface friction between this layer of resin and the adherend onto which it is moulded, hampers the onset of viscoelastic heating [8] and hence bulk heat generation within the layer. This leads to an unbalanced situation in which one of the adherends is overheated even before the resin on the surface of the other substrate starts to melt. This result emphasizes the importance of surface friction when flat energy directors (or energy directors with flat sections) are used at the welding interface.

Finally, the maximum power, vibration time and welding energy were compared for the flat and 4T energy directors. The 4TM energy directors were left out of this comparison owing to their low LSS values and abnormal fracture surfaces. Apart from the baseline combination of welding force and amplitude used so far in this work, i.e. 500 N and 86.2 µm, another set of parameters, namely 300 N and 51.8 µm, was studied. This new set of welding force and amplitude was chosen based on previous results [2] according to which decreasing of the welding force and amplitude causes a significant increase in the time needed to melt the energy director owing to decreased surface friction. The optimum travel values for the flat energy director and the 4T energy director under the new set of welding force and amplitude were defined using the procedure outlined in [3] and validated in the present paper. This led to the same optimum travel values as obtained for the baseline parameters, i.e. 0.30 mm for the flat energy director (LSS 39.0±0.5 MPa) and 0.73 mm for the 4T energy director (LSS

39.1±2.3 MPa). The results shown in Figure 11 indicate that at 500 N and 86.2 µm there are not significant differences between the maximum power, vibration time and welding energy used for the flat and the 4T energy directors. This means that using the flat energy director solution in those conditions does not have any negative influence in the output of the process. However, when both the welding force and the amplitude are reduced to 300 N and 51.8 µm, respectively, the 4T energy director offers significant reductions in maximum power, vibration time and welding energy. This is believed to be related to the fact that, as explained in [2], the time needed for heating and progressively melting of the flat energy director (stages 1_F and 2_F in Fig. 4) increases significantly when both the welding force and amplitude are decreased due to less efficient heat generation through surface friction. Consequently, the preheating effect of the triangular ridges during stages A_{4T} and B_{4T}, as discussed in this paper, has a bigger impact on the overall vibration and, therefore, welding time in the case of low force and amplitude than when force and amplitude are high.

4. Conclusions

A study on flat versus triangular energy directors for the ultrasonic welding of CF/PPS individual samples in a single-lap configuration was carried out. The power and displacement curves provided by the ultrasonic welder when flat energy directors were used showed the same features as the curves obtained in previous work for CF/PEI composites with flat energy directors. Likewise, optimum travel values which led to highest apparent lap shear strength levels and low scatter were easily defined from the power and displacement curves following the procedure established in previous work for CF/PEI composites. In the case of 4T energy directors, i.e. resin stripes with moulded triangles on top, two new stages were found in the power and displacement curves corresponding to heating and progressive melting and flow of

the triangular ridges. After that, the power and displacement curves were quite similar to the ones obtained for flat energy directors and could be used in the same way to define optimum travel values. Optimum lap shear strength, welding energy, maximum dissipated power and vibration time were similar for the flat and 4T energy director solutions for the baseline welding force and amplitude combination, i.e. medium force and high amplitude combination. However, when a combination of low welding force and low amplitude was used, the 4T energy director solution showed decreased power, time and energy as compared to the flat energy director. This was attributed to less efficient heat generation through surface friction in the flat energy director for those specific welding conditions. Finally, moulding of the triangular ridges on top of the adherends for the 4TM energy director solution proved to be challenging. The welding process seemed to be hindered by the presence of a thin moulded layer of resin between the adherend and the triangular ridges and the poor quality of the energy directors affected the power curves to the extent that they could not be interpreted based on the knowledge obtained from the flat energy director case.

In essence, for the material and welding geometry considered in this study, flat energy directors offer simplified processing as compared to more traditional solutions with no significant negative impact in the output of the welding process, unless the required force and amplitude are low. Surface friction plays a major role in heat generation when flat energy directors are used. Therefore, hard constraints to the relative movement between the flat energy director and the adherends might have a negative influence in the welding process.

Acknowledgments

The authors would like to thank Ten Cate Advanced Composites in The Netherlands for supporting this research.

References

1. Benatar A, Gutowski T. Ultrasonic welding of PEEK graphite APC-2 composites. Polym Eng Sci. 1989; 29 (23):1705-1721.
2. Villegas IF. In situ monitoring of ultrasonic welding of thermoplastic composites through power and displacement data. J Thermoplast Compos. 2015; 28(1):66-85.
3. Villegas IF. Strength development versus process data in ultrasonic welding of thermoplastic composites with flat energy directors and its application to the definition of optimum processing parameters. Compos Part A-Appl S. 2014; 65: 27-37
4. Potente H. Ultrasonic welding, principles and theory. Mater Design. 1984; 5(5): 228-234.
5. Villegas IF et al. Process and performance evaluation of ultrasonic, induction and resistance welding of advanced thermoplastic composites. J Thermoplast Compos. 2012; 26(8):1007-1024.
6. Villegas IF, Bersee HEN. Ultrasonic welding of thermoplastic composites: an investigation on energy directing surfaces. Adv Polym Tech. 2010; 29 (2): 112-121.
7. Levy A, Le Corre S, Villegas IF. Modelling of the heating phenomena in ultrasonic welding of thermoplastic composites with flat energy directors. J Mater Process Tech. 2014; 214: 1361-1371.
8. Zhang Z et al. Study on heating process for ultrasonic welding of thermoplastics. J Thermoplast Compos. 2010; 23(5): 647-664.

This is an Accepted Manuscript of an article published by Taylor & Francis in Composite Interfaces in 2015, available online: http://dx.doi.org/10.1080/09276440.2015.1053753

Figure 1. Types of energy directors used in this study. Left: four triangular ridges moulded on bottom substrate (4TM); middle: four triangular ridges moulded on a loose resin stripe (4T); right: flat energy director (F)

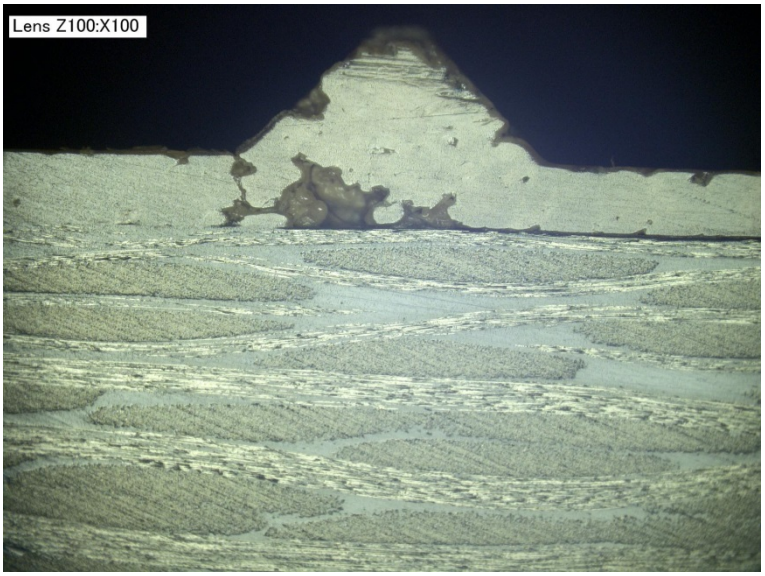

Figure 2. Cross-section micrograph of a triangular energy director moulded on the surface of a composite adherend.

This is an Accepted Manuscript of an article published by Taylor & Francis in Composite Interfaces in 2015, available online: http://dx.doi.org/10.1080/09276440.2015.1053753

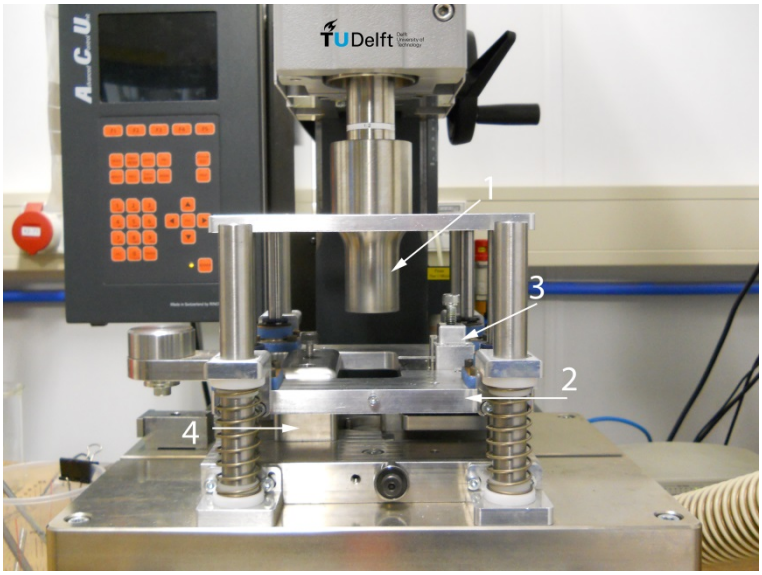

Figure 3. Ultrasonic welding set-up with custom-made jig: (1) sonotrode, (2) support for top adherend, (3) clamp for top adherend, (4) clamp for bottom adherend.

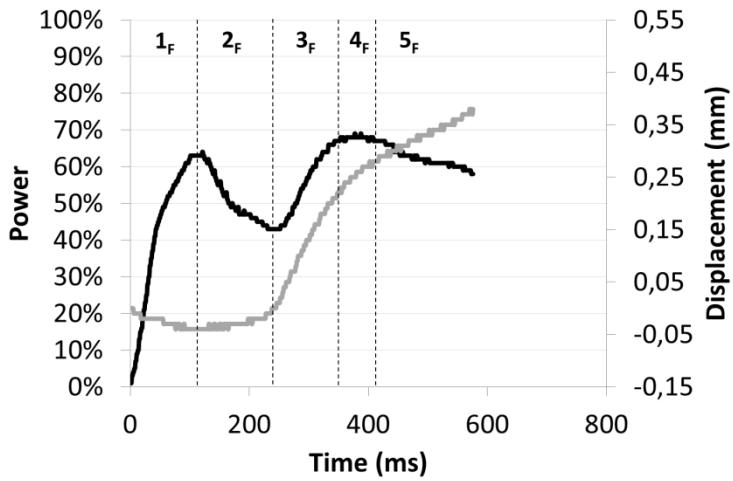

Figure 4. Power (black) and displacement (grey) curves for ultrasonic welding with flat energy directors and different stages in the vibration phase of the welding process.

This is an Accepted Manuscript of an article published by Taylor & Francis in Composite Interfaces in 2015, available online: http://dx.doi.org/10.1080/09276440.2015.1053753

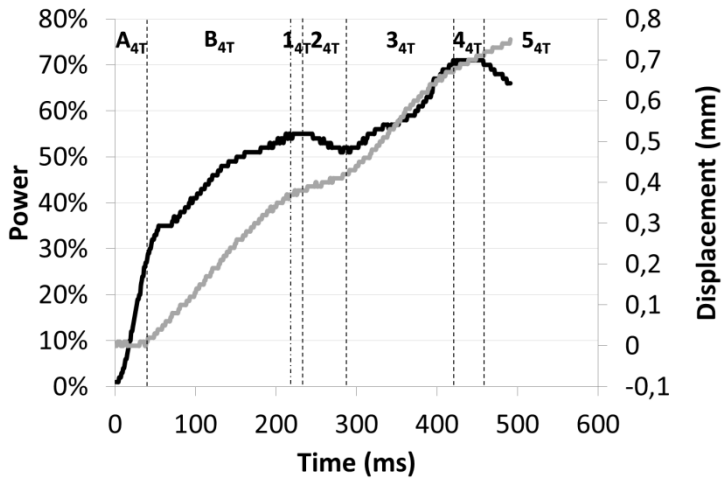

Figure 5. Power (black) and displacement (grey) curves for ultrasonic welding with 4T energy directors and different stages in the vibration phase of the welding process.

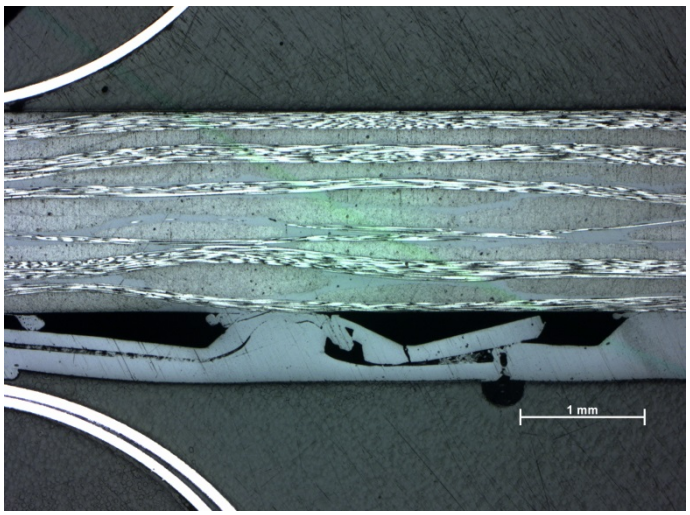

Figure 6. Cross-section micrograph of the top adherend in ultrasonic welding with 4T energy directors interrupted towards the middle of stage B_{4T} (0.2 mm displacement). Melting of the tips of the triangles, layer separation in the energy directors and no adherence to the bottom adherence can be observed.

This is an Accepted Manuscript of an article published by Taylor & Francis in Composite Interfaces in 2015, available online: http://dx.doi.org/10.1080/09276440.2015.1053753

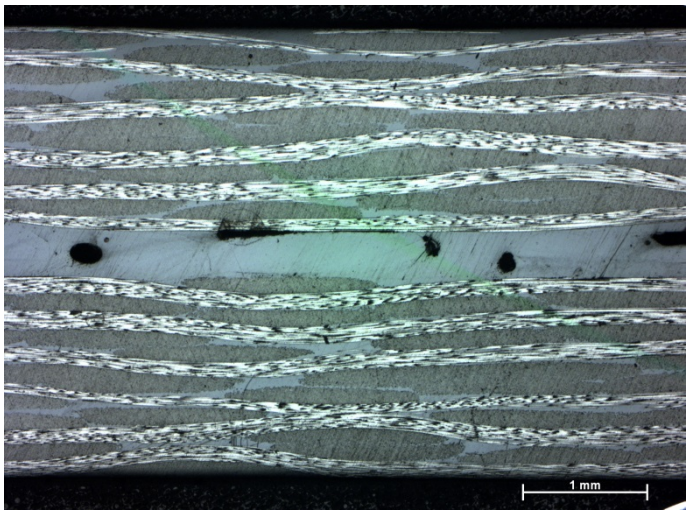

Figure 7. Cross-section micrograph of a 4T energy-director weld interrupted towards the end of stage B_{4T} (0.3 mm displacement). Almost full re-consolidation of the energy director and filling in of the space between the adherends has been achieved.

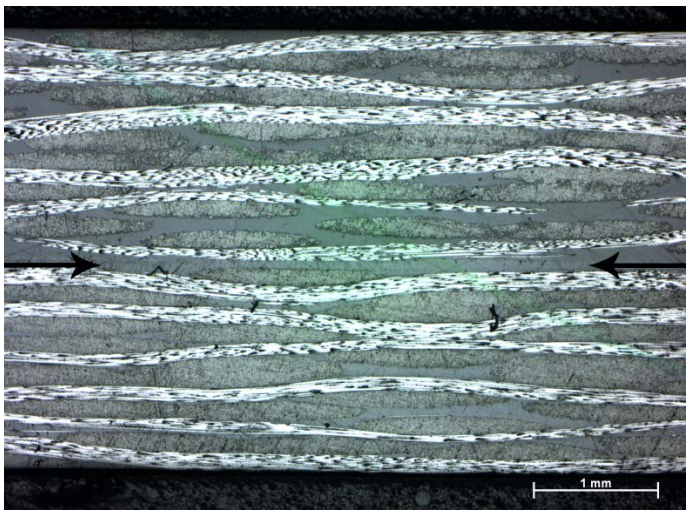

Figure 8. Cross-section micrograph of a 4T energy-director weld interrupted towards the end of stage 3_{4T} (0.6 mm displacement). Thickness of the weldline (indicated by arrows) has significantly decreased; no voids or gaps can be observed at the weldline.

This is an Accepted Manuscript of an article published by Taylor & Francis in Composite Interfaces in 2015, available online: http://dx.doi.org/10.1080/09276440.2015.1053753

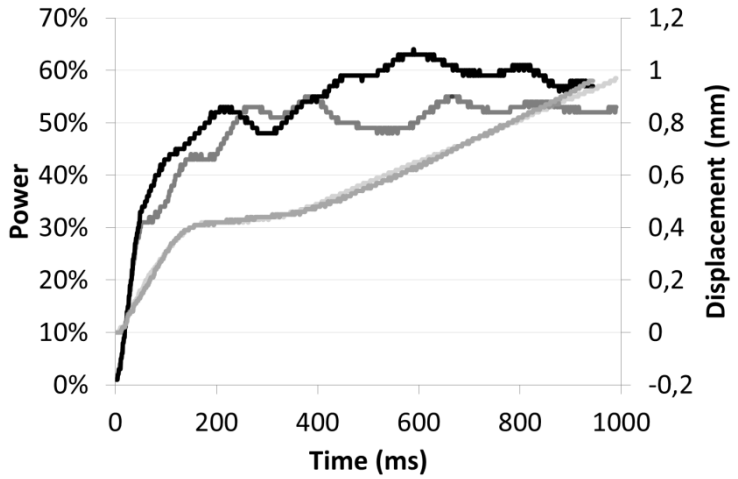

Figure 9. Power and displacement curves for two different samples with 4TM energy directors.

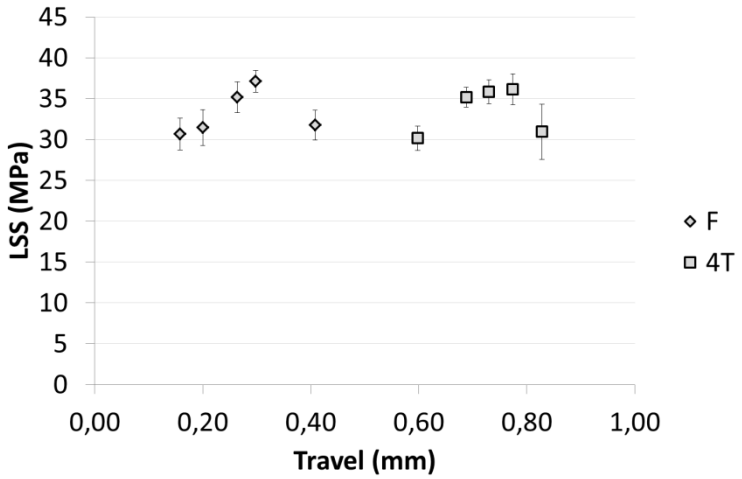

Figure 10. LSS versus travel for flat (F) and 4T energy directors

This is an Accepted Manuscript of an article published by Taylor & Francis in Composite Interfaces in 2015, available online: http://dx.doi.org/10.1080/09276440.2015.1053753

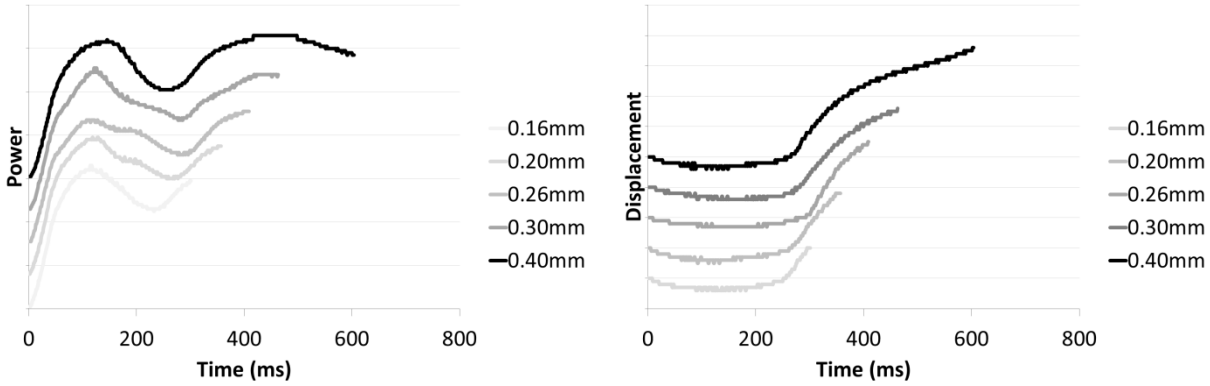

Figure 11. Representative power (left) and displacement (right) curves for the travel values considered for mechanical tests (flat energy director). Curves as shifted upwards for improved clarity.

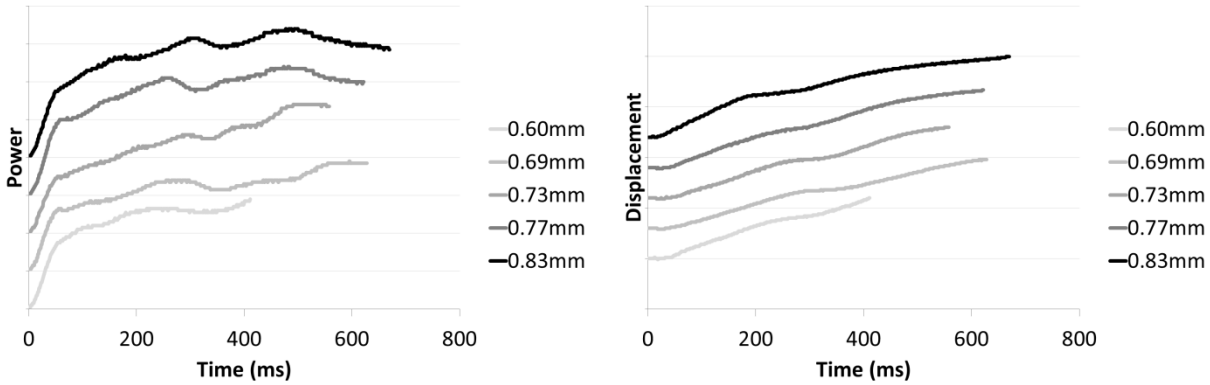

Figure 12. Representative power (left) and displacement (right) curves for the travel values considered for mechanical tests (4T energy director). Curves are shifted upwards for improved clarity.

This is an Accepted Manuscript of an article published by Taylor & Francis in Composite Interfaces in 2015, available online: http://dx.doi.org/10.1080/09276440.2015.1053753

Figure 13. Mating fracture surfaces for a 4TM welded sample with 0.75 mm travel: bottom adherend (right), top adherend (left)

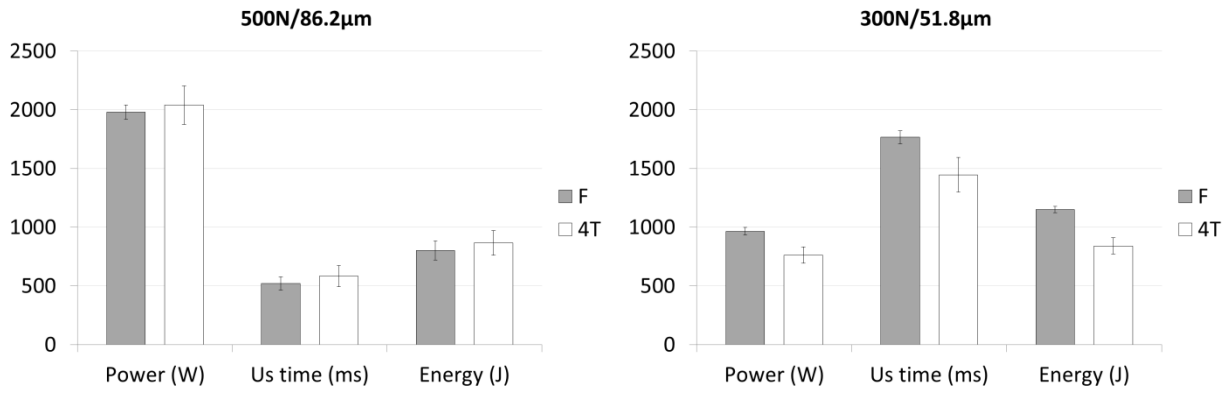

Figure 14. Maximum power, vibration time and welding energy for two different sets of welding parameters (force and amplitude) and two types of energy director (flat, F, and 4T).

This is an Accepted Manuscript of an article published by Taylor & Francis in Composite Interfaces in 2015, available online: http://dx.doi.org/10.1080/09276440.2015.1053753

Table 1. Processing conditions and geometric features of the different types of energy directors in this study

ED type	**Material**	**Temperature (°C)**	**Pressure (bar)**	**Time @ processing T (min)**	**Thickness of flat part of ED (mm)**	**Height of triangular ridges (mm)**
F	Resin film (0.08 mm thick) – 5 layers	260	20	10	0.4	-
4T	Resin film (0.08 mm thick) – 5 layers	260	20	10	0.4	0.5
4TM	Resin powder	275	10	30	0.42	0.55